

## **Investigations on Chemical Interactions between Alternate Cathodes and Lanthanum Gallate Electrolyte for Intermediate Temperature Solid Oxide Fuel Cell (ITSOFC)**

A. Samson Nesaraj\*, M. Kumar, I. Arul Raj, I. Radhakrishna and R. Pattabiraman

*\*Department of Chemistry, Karunya University, Coimbatore-641 114, India*

*Central Electrochemical Research Institute, Karaikudi-630 006, India*

*(Received 10 February 2006, Accepted 25 October 2006)*

The doped perovskite oxides such as  $\text{La}_{0.65}\text{Sr}_{0.30}\text{MnO}_{3-\delta}$  (LSM),  $\text{La}_{0.70}\text{Sr}_{0.30}\text{CoO}_{3-\delta}$  (LSC),  $\text{La}_{0.65}\text{Sr}_{0.30}\text{FeO}_{3-\delta}$  (LSF),  $\text{La}_{0.65}\text{Sr}_{0.30}\text{NiO}_{3-\delta}$  (LSN) and  $\text{La}_{0.60}\text{Sr}_{0.40}\text{Co}_{0.20}\text{Fe}_{0.80}\text{O}_{3-\delta}$  (LSCF) are proposed as alternate cathode materials for solid oxide fuel cells working at reduced temperature (< 1073 K). The critical requirement for their applicability is their chemical compatibility in conjunction with an alternate solid electrolyte,  $\text{La}_{0.9}\text{Sr}_{0.1}\text{Ga}_{0.8}\text{Mg}_{0.2}\text{O}_{3-\delta}$  (LSGM) without any new phase formation. To understand the chemical reactivity between these two components, thoroughly mixed different cathode and LSGM electrolyte (1:1 by wt.) powders were pressed as circular components and subjected to annealing at 1573 K for 3 h in air. XRD and SEM were used for the characterization of the annealed samples. XRD measurements revealed that no new secondary phases were formed in LSM, LSC, and LSF with LSGM mixtures whereas LSN and LSCF with LSGM resulted in the formation of new secondary phases after high temperature treatment. The sintering shrinkage for all the components (cathode + electrolyte mixture) was also estimated. For comparison of data, the individual powders (cathode/electrolyte) were also compacted and studied in the same manner. The obtained results are discussed keeping in view the requirements that the candidate cathode material must meet out with respect to its chemical compatibility to qualify for the LSGM based ITSOFC systems at 1073 K.

**Keywords:** Cathode, Electrolyte, Chemical interactions, Solid oxide fuel cell

---

### **INTRODUCTION**

Solid oxide fuel cells have several distinct advantages over other types of fuel cells including use of non-precious materials, no liquids involved in the fuel cell and invariant electrolyte. The use of solid electrolytes in ceramic fuel cells eliminates material corrosion and electrolyte management problems. The high operating temperature promotes rapid reaction kinetics, allows reforming of hydrocarbon fuels (natural gas, coal gas, bio-gas) within the fuel cell and

produces heat suitable for co-generation. Furthermore, because all the components are solid, ceramic fuel cells can be fabricated in very thin layers, and cell components can be configured into shapes which are unachievable in fuel cell systems having a liquid electrolyte [1-3].

The major problems associated with high temperature SOFC are severe restrictions on the choice of materials, electrode sintering, interfacial diffusion between electrode and electrolyte and mechanical stress due to different thermal expansion coefficients. Another major problem reported in this device is the thermal mismatch of the components at the operation temperature [4]. Although, a solid oxide fuel cell is

---

\*Corresponding author. E-mail: drsamson@karunya.edu

an all ceramic device, the inherent difficulties posed by the right choice of materials and the right techniques employed for their fabrication into thin sections of large area components with reproducible characteristics remain to be solved yet. The primary advantages for lowering the operating temperature of SOFC below 1073 K are to arrive at an optimum between performance and life time of the stack and to reduce the overall system cost [5].

Since Ishihara's discovery of high ionic conduction by  $\text{La}_{0.9}\text{Sr}_{0.1}\text{Ga}_{0.8}\text{Mg}_{0.2}\text{O}_{3-\delta}$ , partially substituted  $\text{LaGaO}_3$  was proposed as the one of the alternate electrolytes for ITSOFC application [6]. However, there are still many problems to be solved in order to use this material commercially. Another important issue of importance in SOFC technology is the selection of appropriate ceramic electrocatalysts for the cathode. The cathode must meet certain requirements, such as high electronic conductivity, high catalytic activity for oxygen reduction, chemical as well as thermal expansion compatibility with the electrolyte, no destructive phase formation within the operating temperature range and controllable sintering behavior [3]. Ceramic electrodes based on the lanthanum manganites partially substituted with 'Sr' have been widely studied, particularly for use in SOFCs using yttria stabilized zirconia (YSZ) as electrolyte material. The main problem concerning these materials lies with the formation of interfacial phases between the electrode and the electrolyte, which are detrimental for the conductivity in the boundary [7-11]. As alternate to the lanthanum manganites many other perovskite compounds have been developed especially for ITSOFC cathode application.

However, for the operation of ITSOFCs to be technically feasible, two parameters should be considered: 1) the development of high performance electrodes, because the electrode reaction rates decrease at reduced temperature and 2) the minimization of cell resistance. The later means minimization of ohmic loss at the electrolyte-electrode interfaces [12]. The state-of-the cathode with new composition ( $\text{La}_{0.65}\text{Sr}_{0.30}\text{MnO}_{3-\delta}$ ) was chosen in this study, since it showed no reaction products with YSZ electrolyte for prolonged duration in SOFC [13]. Also, doped perovskite oxides such as  $\text{La}_{0.65}\text{Sr}_{0.30}\text{FeO}_{3-\delta}$ ,  $\text{La}_{0.70}\text{Sr}_{0.30}\text{CoO}_{3-\delta}$ ,  $\text{La}_{0.65}\text{Sr}_{0.30}\text{NiO}_{3-\delta}$ , and  $\text{La}_{0.60}\text{Sr}_{0.40}\text{Co}_{0.20}\text{Fe}_{0.80}\text{O}_{3-\delta}$  were also examined as alternate cathode materials in this study for ITSOFC application [14].

The crucial requirement for the application of these materials is their chemical compatibility in conjunction with the solid electrolyte without any new phase formation.  $\text{La}_{0.9}\text{Sr}_{0.1}\text{Ga}_{0.8}\text{Mg}_{0.2}\text{O}_{3-\delta}$  was adopted as an electrolyte due to its highest oxide ion conductivity at reduced temperatures for SOFC application [15-16]. The chemical compatibility studies between alternate cathode materials and LSGM based electrolyte is reported in this research article.

## EXPERIMENTAL

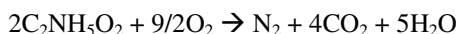
### Sample Preparation by Self Propagating Combustion Synthesis

The cathode materials such as,  $\text{La}_{0.65}\text{Sr}_{0.30}\text{MnO}_{3-\delta}$ ,  $\text{La}_{0.65}\text{Sr}_{0.30}\text{FeO}_{3-\delta}$ ,  $\text{La}_{0.70}\text{Sr}_{0.30}\text{CoO}_{3-\delta}$ ,  $\text{La}_{0.65}\text{Sr}_{0.30}\text{NiO}_{3-\delta}$  and  $\text{La}_{0.60}\text{Sr}_{0.40}\text{Co}_{0.20}\text{Fe}_{0.80}\text{O}_{3-\delta}$  and novel electrolyte,  $\text{La}_{0.9}\text{Sr}_{0.1}\text{Ga}_{0.8}\text{Mg}_{0.2}\text{O}_{3-\delta}$ , were prepared by the combustion synthesis process using glycine as a fuel. The combustion method involves the combustion of saturated aqueous solution containing stoichiometric quantities of the corresponding nitrates (oxidizers) and glycine ( $\text{NH}_2\text{-CH}_2\text{COOH}$ ) fuel. The appropriate quantities of the precursor nitrate salts (if oxide/acetate salts were taken, they were converted as nitrates by treating them with nitric acid) were calculated according to the concepts of propellant chemistry [17-18], taken in quartz crucible and dissolved in triple distilled water. Calculated amount of glycine (fuel and complexant) was added to the above solution with continuous stirring and homogenized well. The appropriate amounts of the reactants taken for combustion synthesis with glycine fuel are indicated in Table 1. The oxidizer:fuel ratio was calculated based on oxidizing (O) and fuel (F) valencies of the reactants keeping  $\text{O/F} = 1$  as reported [19-20]. The aqueous redox solution containing metal nitrates and glycine when introduced into a muffle furnace preheated to 823 K, boils, froths, ignites and catches fire (at a high temperature  $1373 \pm 100$  K). At this temperature the metal nitrates decompose to metal oxides and oxides of nitrogen and hence act as oxidizer for further combustion, which leads to a voluminous, foamy combustion residue in less than 5 min. The flame persisted for about 1 min. The foam was then lightly ground in a glass basin with porcelain pestle to obtain fine powders. The procedure is explained schematically in Fig. 1. When glycine is used as fuel, the following reaction take

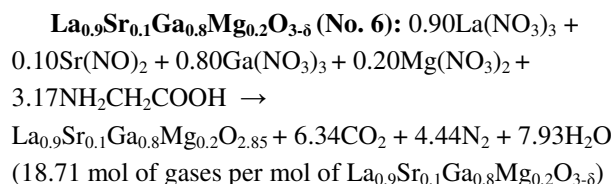
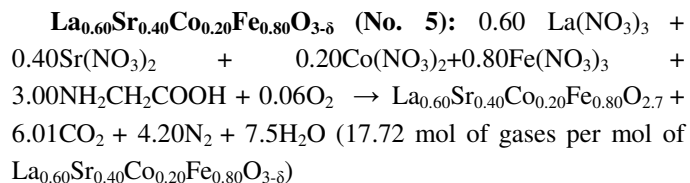
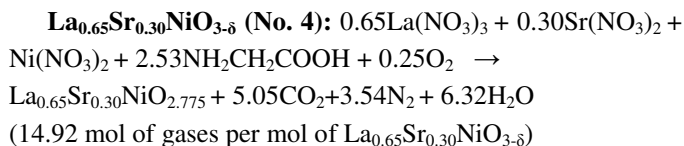
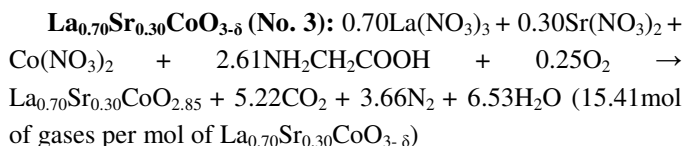
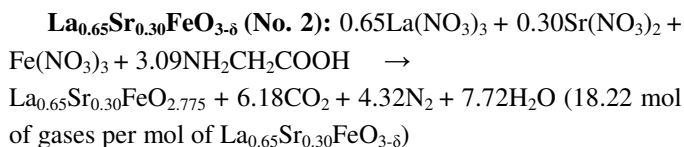
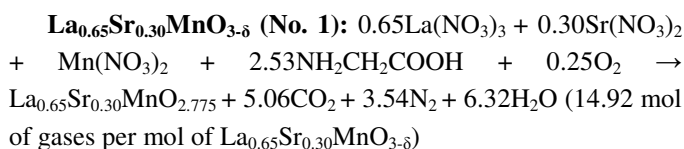
**Table 1.** Amount of Precursor Materials Taken for Combustion Synthesis of Different Cathode/Electrolyte Powders

Sample	La(NO <sub>3</sub> ) <sub>3</sub> (g)	La <sub>2</sub> O <sub>3</sub> (g)	Sr(NO <sub>3</sub> ) <sub>2</sub> (g)	Ga(NO <sub>3</sub> ) <sub>3</sub> (g)	Mg(NO <sub>3</sub> ) <sub>2</sub> (g)	Manganese acetate (g)	Fe(NO <sub>3</sub> ) <sub>3</sub> (g)	Co(NO <sub>3</sub> ) <sub>2</sub> (g)	Ni(NO <sub>3</sub> ) <sub>2</sub> (g)	Glycine (g)
(No. 1)	14.07		3.17	-	-	12.25	-	-	-	40.00
(No. 2)	14.07	-	3.17	-	-	-	20.2	-	-	40.00
(No. 3)	15.15	-	3.17	-	-	-	-	14.55	-	40.00
(No. 4)	14.07	-	3.17	-	-	-	-	-	14.54	40.00
(No. 5)	12.99	-	4.23	-	-	-	16.16	2.91	-	40.00
(No. 6)	-	2.93	0.42	6.68	1.02	-	-	-	-	20.00

place. One mole of glycine gives 5 moles of gases, as:



The stoichiometric redox reaction between metal nitrates and glycine to obtain cathode/electrolyte powders from combustion reaction can be represented by the following theoretical equations:



Calcination of the as-synthesized powders was carried out in clean alumina crucibles between 1073-1173 K for 6 h in air to remove the deposited carbon and the unreacted organic residues to get phase pure compounds [18]. The heat treated cathode/electrolyte powders were characterized by JEOL-8030 X-ray diffractometer with 2 $\theta$  scan mode at an operating rate of 40 KV, 20 mA; the characteristic X-radiation was CuK $\alpha$  (Ni filter) possessing the wavelength,  $\lambda = 1.5418\text{\AA}$ .

### Reaction Experiments

The La<sub>0.65</sub>Sr<sub>0.30</sub>MnO<sub>3- $\delta$</sub> /La<sub>0.65</sub>Sr<sub>0.30</sub>FeO<sub>3- $\delta$</sub> /La<sub>0.70</sub>Sr<sub>0.30</sub>CoO<sub>3- $\delta$</sub> /La<sub>0.65</sub>Sr<sub>0.30</sub>NiO<sub>3- $\delta$</sub> /La<sub>0.60</sub>Sr<sub>0.40</sub>Co<sub>0.20</sub>Fe<sub>0.80</sub>O<sub>3- $\delta$</sub>  cathode and La<sub>0.9</sub>Sr<sub>0.1</sub>Ga<sub>0.8</sub>Mg<sub>0.2</sub>O<sub>3- $\delta$</sub>  electrolyte powders were mixed individually in a 1:1 weight ratio, together in a pestle and mortar. Powder mixtures with 1:1 wt. ratio were chosen because they may give good results after high temperature

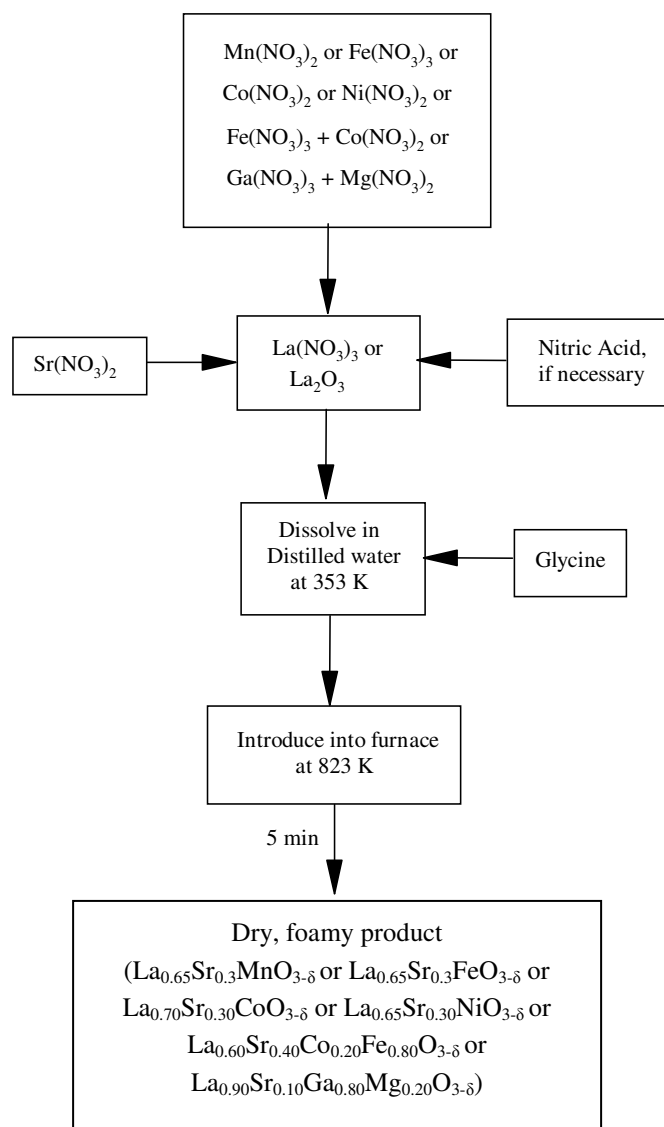


**Fig. 1.** Flow chart to prepare cathode/electrolyte materials by combustion synthesis.

annealing. Each powder mixture (cathode + electrolyte) was ground well, placed in a 20 mm diameter die, compacted with an uniaxial hydraulic pressing machine at a load of 156 Mpa. Each pellet was then annealed in air at 1573 K for 3 h in a rapid heating furnace with a heating/cooling rate of 20 °C min<sup>-1</sup>. A temperature of 1573 K was selected for the chemical compatibility tests, because, although the operating

temperature of the cell is substantially less, the steps involved in the fabrication of ceramic cathode/electrolyte/electrode structures usually require processing up to at least 1473 K [21-22]. The calcined pellets were crushed into powder form and the reaction products were identified by X-ray Diffraction study. Prior to XRD, the microstructures of the annealed samples were investigated by Scanning Electron Microscopy (using S-3000 H, Hitachi Scanning Electron Microscope at an acceleration voltage of 20 kV). For comparison of results, the individual cathode/electrolyte powders were also compacted and studied separately in the same manner.

## RESULTS AND DISCUSSION

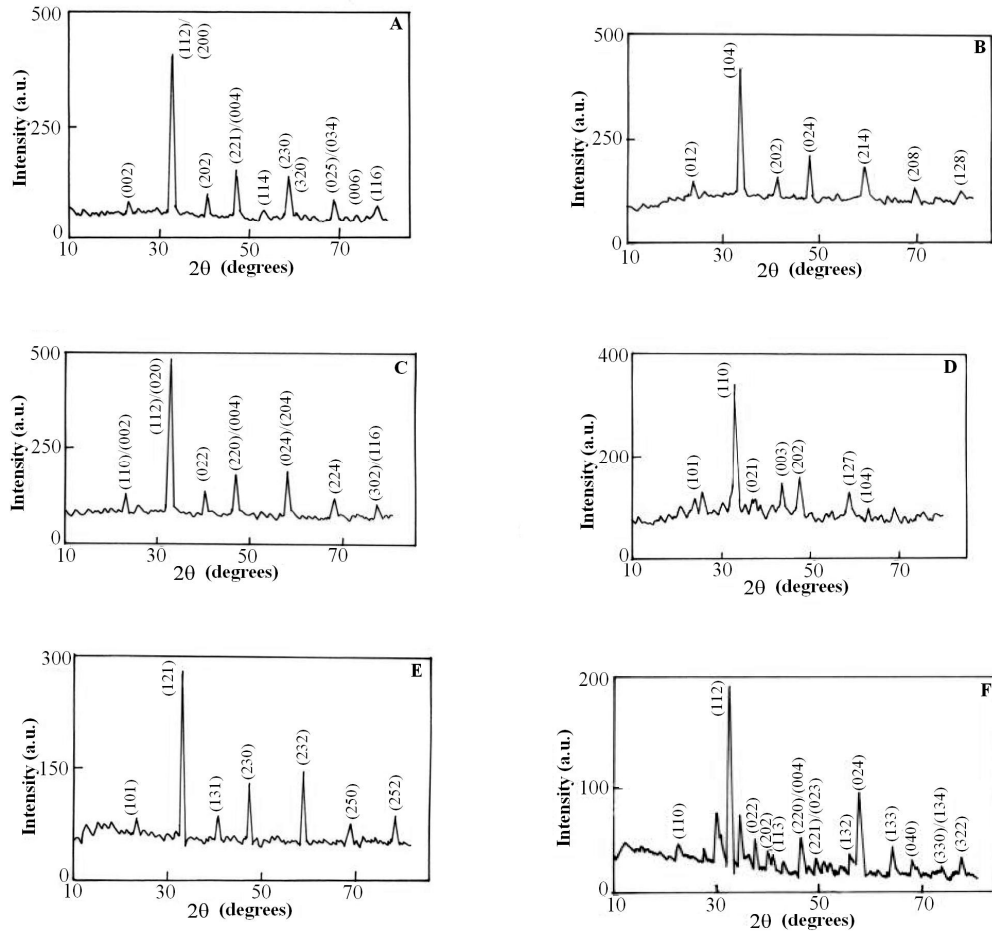
### Characterization of Cathode and Electrolyte Powders by XRD Technique

Figure 2 shows the XRD patterns obtained for  $\text{La}_{0.65}\text{Sr}_{0.30}\text{MnO}_{3-\delta}$ ,  $\text{La}_{0.65}\text{Sr}_{0.30}\text{FeO}_{3-\delta}$ ,  $\text{La}_{0.70}\text{Sr}_{0.30}\text{CoO}_{3-\delta}$ ,  $\text{La}_{0.65}\text{Sr}_{0.30}\text{NiO}_{3-\delta}$ ,  $\text{La}_{0.60}\text{Sr}_{0.40}\text{Co}_{0.20}\text{Fe}_{0.80}\text{O}_{3-\delta}$ , and  $\text{La}_{0.9}\text{Sr}_{0.1}\text{Ga}_{0.8}\text{Mg}_{0.2}\text{O}_{3-\delta}$ . The lattice parameters for cathode/electrolyte powders were calculated by least square fitting method using DOS computer programming. The obtained lattice parameters are in good agreement with the reported JCPDS data. A comparison between the obtained crystallographic parameters with the corresponding standard JCPDS data has been made in Table 2.

### Sintering Characteristics

The annealing data obtained on circular individual (cathode and electrolyte) pellets are shown in Tables 3 and 4. The annealing data obtained on circular pellets of cathodes ( $\text{La}_{0.65}\text{Sr}_{0.30}\text{MnO}_{3-\delta}/\text{La}_{0.65}\text{Sr}_{0.30}\text{FeO}_{3-\delta}/\text{La}_{0.70}\text{Sr}_{0.30}\text{CoO}_{3-\delta}/\text{La}_{0.65}\text{Sr}_{0.30}\text{NiO}_{3-\delta}/\text{La}_{0.60}\text{Sr}_{0.40}\text{Co}_{0.20}\text{Fe}_{0.80}\text{O}_{3-\delta}$ ) mixed with  $\text{La}_{0.9}\text{Sr}_{0.1}\text{Ga}_{0.8}\text{Mg}_{0.2}\text{O}_{3-\delta}$  electrolyte (1:1 by wt.) is shown in Tables 5 and 6.

Diffusion of ions leading to a solid-state reaction between cathode and electrolyte materials is known to be responsible for the degradation of SOFCs [10-11]. During the fabrication as well as the operation of SOFCs, the high temperature produced at the interfaces results in inter-diffusion of ions and, consequently, in the formation of insulating phases that are thermodynamically feasible under those conditions. In order to



**Fig. 2.** XRD patterns obtained for different cathode and electrolyte powders: (A)  $\text{La}_{0.65}\text{Sr}_{0.30}\text{MnO}_{3-\delta}$  cathode, (B)  $\text{La}_{0.65}\text{Sr}_{0.30}\text{FeO}_{3-\delta}$  cathode, (C)  $\text{La}_{0.70}\text{Sr}_{0.30}\text{CoO}_{3-\delta}$  cathode, (D)  $\text{La}_{0.65}\text{Sr}_{0.30}\text{NiO}_{3-\delta}$  cathode, (E)  $\text{La}_{0.60}\text{Sr}_{0.40}\text{Co}_{0.20}\text{Fe}_{0.80}\text{O}_{3-\delta}$  cathode, (F)  $\text{La}_{0.9}\text{Sr}_{0.1}\text{Ga}_{0.8}\text{Mg}_{0.2}\text{O}_{3-\delta}$  electrolyte.

clarify the effects on annealing, the densification details of compacts (made from individual cathodes, LSGM electrolyte and combined cathode + LSGM electrolyte) were studied. After annealing at 1573 K for 3 h, the compacts exhibited different sintering characteristics. From Tables 3 and 4, it is understood that LSM cathode exhibited 100% densification at 1573 K. Other cathodes exhibited lower densification values at 1573 K. LSGM electrolyte exhibited 80.82% of densification at 1573 K. From Tables 5 and 6, it is seen that the cathode material in the cathode + electrolyte mixture plays a main role in influencing the final density of a particular compact. In

general, sintering of ceramics depends on heating temperature and holding time. From Table 6, it is seen that the LSM + LSGM compact exhibited higher percent of shrinkage (42.47%) after sintering at 1573 K. Among the five type of pellets made from cathode + electrolyte mixture, the compact made from LSN + LSGM exhibited a very low percent of shrinkage (12.62%) after sintering at 1573 K. From the densification data, it is found that the LSM + LSGM pellet has exhibited 63.68% of densification (which is higher than the others) after sintering at 1573 K. Like the shrinkage data, the LSN + LSGM compact has shown very low densification, i.e.,

**Table 2.** Comparison of Crystallographic Parameters with Standard JCPDS Data

Sl. No	Properties/ cathode/electrolyte powder	Crystal structure	Unit cell parameters (Å)	Unit cell volume (Å <sup>3</sup> )
1	Standard XRD data LaMnO <sub>3</sub> (JCPDS No. 33-713)	Orthorhombic	a = 5.5320 b = 5.7220 c = 7.6990	243.7049
	Obtained XRD data for La <sub>0.65</sub> Sr <sub>0.30</sub> MnO <sub>3-δ</sub> powder	Orthorhombic	a = 5.4072 b = 5.8044 c = 7.6924	241.4364
2	Standard XRD data for LaFeO <sub>3</sub> powder (JCPDS No. 37-1493)	Orthorhombic	a = 5.5320 b = 7.8350 c = 5.5530	240.6849
	Obtained XRD data for La <sub>0.65</sub> Sr <sub>0.30</sub> FeO <sub>3-δ</sub> powder	Orthorhombic	a = 5.6133 b = 7.7592 c = 5.4882	239.0369
3	Standard XRD data for La <sub>0.60</sub> Sr <sub>0.40</sub> CoO <sub>3-δ</sub> powder (JCPDS No. 36-1393)	Rhombohedral -hexagonal	a = 5.4270 c = 13.2180	337.1345
	Obtained XRD data for La <sub>0.70</sub> Sr <sub>0.30</sub> CoO <sub>3-δ</sub> powder	Rhombohedral -hexagonal	a = 5.3767 c = 13.2576	331.9183
4	Standard XRD data for LaNiO <sub>3</sub> powder (JCPDS No.33-711)	Rhombohedral -hexagonal	a = 5.4570 c = 6.5720	169.4819
	Obtained XRD data for La <sub>0.65</sub> Sr <sub>0.30</sub> NiO <sub>3-δ</sub> powder	Rhombohedral -hexagonal	a = 5.6210 c = 6.1776	169.0304
5	Standard XRD data for LaFeO <sub>3</sub> powder (JCPDS No. 37-1493)	Orthorhombic	a = 5.5669 b = 7.7847 c = 5.5330	247.2656
	Obtained XRD data for La <sub>0.60</sub> Sr <sub>0.40</sub> Co <sub>0.20</sub> Fe <sub>0.80</sub> O <sub>3-δ</sub> powder	Orthorhombic	a = 5.6576 b = 7.8837 c = 5.4939	245.0434
6	Standard XRD data for LaGaO <sub>3</sub> Powder (JCPDS No. 24-1102)	Orthorhombic	a = 5.4870 b = 5.5200 c = 7.7520	234.7944
	Obtained XRD data for La <sub>0.9</sub> Sr <sub>0.1</sub> Ga <sub>0.8</sub> Mg <sub>0.2</sub> O <sub>3-δ</sub> Powder	Orthorhombic	a = 5.3741 b = 5.5433 c = 7.9145	235.7749

**Table 3.** Annealing Data Obtained on Circular Pellets of Individual Cathode and Electrolyte Materials

Sample identity	Height (cm)	Radius (cm)	Volume (cc)	Wt. (g)	Density (g cc <sup>-1</sup> )	Annealing temperature (K)	Height (cm)	Radius (cm)	Volume (cc)	Wt. (g)	Density (g cc <sup>-1</sup> )
LSM	0.144	1.0	0.452	0.945	2.091	1573	0.102	0.750	0.180	0.895	4.972
LSF	0.097	1.0	0.305	0.925	3.033	1573	0.106	0.903	0.271	0.905	3.339
LSC	0.090	1.0	0.283	0.925	3.269	1573	0.075	0.815	0.156	0.885	5.673
LSN	0.093	1.0	0.292	0.940	3.219	1573	0.086	0.840	0.191	0.900	4.712
LSCF	0.110	1.0	0.345	0.945	2.739	1573	0.103	0.800	0.207	0.930	4.492
LSGM	0.123	1.0	0.386	0.950	2.461	1573	0.111	0.775	0.209	0.930	4.450

**Table 4.** The degree of Change in Volume and Density Obtained on Circular Pellets of Individual Cathode and Electrolyte Pellets as a Function of Annealing Temperature

Sample identity	Volume before annealing (cc)	Density before annealing (g cc <sup>-1</sup> )	Annealing temperature (K)	Volume after annealing (g/cc)	Density after annealing (g/cc)	Reduction in volume (cc)	Shrinkage factor (%)	Increase in density (g cc <sup>-1</sup> )	Densification factor (%)
LSM	0.452	2.091	1573	0.180	4.972	0.272	60.17	2.881	~100.00
LSF	0.305	3.033	1573	0.271	3.339	0.034	11.15	0.306	10.09
LSC	0.283	3.269	1573	0.156	5.673	0.127	44.87	2.404	73.53
LSN	0.292	3.219	1573	0.191	4.712	0.101	34.58	1.493	46.38
LSCF	0.345	2.739	1573	0.201	4.492	0.138	40.00	1.753	64.00
LSGM	0.386	2.494	1573	0.209	4.450	0.177	45.85	1.989	80.82

only 6.10% after sintering at 1573 K. The pellet with higher percent of densification might exhibit close contact with each powder particle, which could give better information on the reaction products when identified by XRD analysis.

### Micro-structural Examination of Individual Cathodes and Electrolyte

The microstructures of different sintered pellets studied are shown in Fig. 3.

**La<sub>0.65</sub>Sr<sub>0.30</sub>MnO<sub>3-δ</sub> cathode.** The microstructure of a sintered La<sub>0.65</sub>Sr<sub>0.30</sub>MnO<sub>3-δ</sub> pellet is shown in Fig. 3A. It presented a dense body with grain sizes varying between 2 to 60 μm. The LSM pellet presented the highest relative density (~100%) when sintered at 1573 K for 3 h. As seen in Fig. 3A, the microstructure consisted of uniform grains of size 50 μm.

No significant pores were observed and all grains were perfectly connected with each other.

**La<sub>0.65</sub>Sr<sub>0.30</sub>FeO<sub>3-δ</sub> cathode.** The microstructure of a sintered La<sub>0.65</sub>Sr<sub>0.30</sub>FeO<sub>3-δ</sub> pellet is shown in Fig. 3B. The LSF compact showed the microstructure of agglomerates with irregular arrangement of particles. Moreover some small pores still exist in the body after sintering at 1473 K. From the micrograph, it is noted that the surface of the pellet was not smooth. The grain sizes are found to be around 10 μm in diameter.

**La<sub>0.70</sub>Sr<sub>0.30</sub>CoO<sub>3-δ</sub> cathode.** The microstructure of a sintered La<sub>0.70</sub>Sr<sub>0.30</sub>CoO<sub>3-δ</sub> pellet is shown in Fig. 3C. It is clear that the microstructure is fairly uniform and no secondary phases are present, which is in consistence with X-ray analysis. The average grain sizes are found to vary between 20

**Table 5.** Annealing Data Obtained on Circular Pellets of ITSOFC Cathodes Mixed with Doped Lanthanum Gallate (LSGM9182) Electrolyte (1:1 by wt.)

Sample identity	Height (cm)	Radius (cm)	Volume (cc)	Wt. (g)	Density (g cc <sup>-1</sup> )	Annealing temperature (K)	Height (cm)	Radius (cm)	Volume (cc)	Wt. (g)	Density (g cc <sup>-1</sup> )
LSM + LSGM	0.222	1.0	0.697	1.89	2.712	1573	0.177	0.850	0.401	1.78	4.439
LSF + LSGM	0.190	1.0	0.597	1.85	3.099	1573	0.171	0.925	0.459	1.81	3.943
LSC + LSGM	0.198	1.0	0.622	1.84	2.958	1573	0.169	0.890	0.420	1.75	4.167
LSN + LSGM	0.222	1.0	0.697	1.92	2.755	1573	0.202	0.980	0.609	1.78	2.923
LSCF + LSGM	0.196	1.0	0.615	1.96	3.187	1573	0.178	0.950	0.504	1.89	3.750

**Table 6.** The Degree of Change in Volume and Density Obtained on Circular Pellets of ITSOFC Cathodes with LSGM9182 Electrolyte (1:1 by wt.) as a Function of Annealing Temperature

Sample identity	Volume before annealing (cc)	Density before annealing (g cc <sup>-1</sup> )	Annealing temperature (K)	Volume after annealing (g cc <sup>-1</sup> )	Density after annealing (g cc <sup>-1</sup> )	Reduction in volume (cc)	Shrinkage factor (%)	Increase in density (g cc <sup>-1</sup> )	Densification factor (%)
LSM + LSGM	0.697	2.712	1573	0.401	4.439	0.296	42.47	1.727	63.68
LSF + LSGM	0.597	3.099	1573	0.459	3.943	0.138	23.11	0.844	27.23
LSC + LSGM	0.622	2.958	1573	0.420	4.167	0.202	32.47	1.209	40.87
LSN + LSGM	0.697	2.755	1573	0.609	2.923	0.088	12.62	0.168	6.10
LSCF + LSGM	0.615	3.187	1573	0.504	3.750	0.111	18.05	0.563	17.66

Investigations on chemical interactions

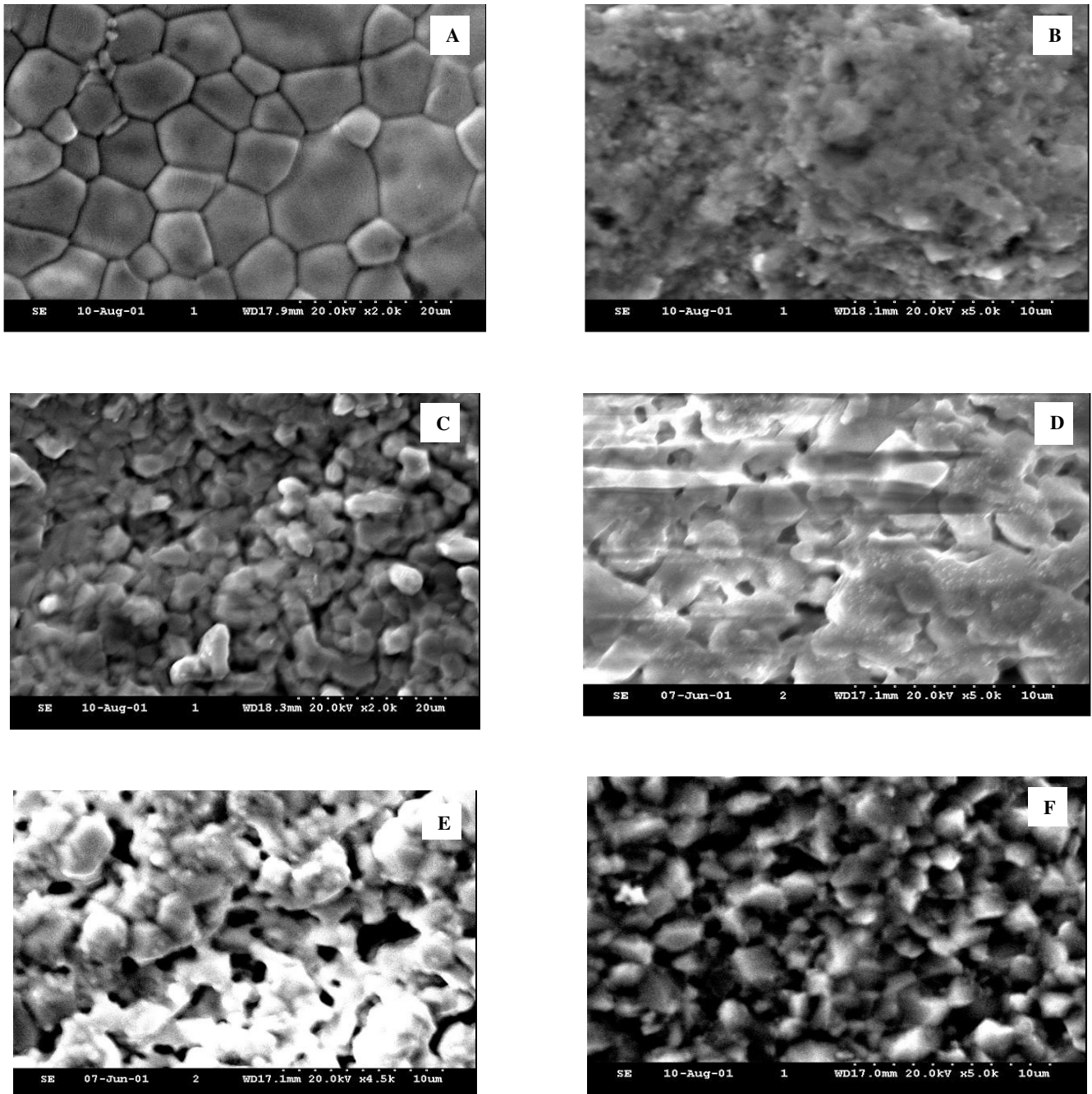


**Fig. 3.** SEM photographs obtained on different sintered electrode and electrolyte specimen: (A)  $\text{La}_{0.65}\text{Sr}_{0.30}\text{MnO}_{3-\delta}$  cathode, (B)  $\text{La}_{0.65}\text{Sr}_{0.30}\text{FeO}_{3-\delta}$  cathode, (C)  $\text{La}_{0.70}\text{Sr}_{0.30}\text{CoO}_{3-\delta}$  cathode, (D)  $\text{La}_{0.65}\text{Sr}_{0.30}\text{NiO}_{3-\delta}$  cathode, (E)  $\text{La}_{0.60}\text{Sr}_{0.40}\text{Co}_{0.20}\text{Fe}_{0.80}\text{O}_{3-\delta}$  cathode, (F)  $\text{La}_{0.90}\text{Sr}_{0.10}\text{Ga}_{0.80}\text{Mg}_{0.20}\text{O}_{3-\delta}$  electrolyte.

to 30  $\mu\text{m}$ . Closed pores observed in this pellet were mainly formed by close-packed grains [23].

**La<sub>0.65</sub>Sr<sub>0.30</sub>NiO<sub>3- $\delta$</sub>  cathode.** The microstructure of a sintered La<sub>0.65</sub>Sr<sub>0.30</sub>NiO<sub>3- $\delta$</sub>  pellet is shown in Fig. 3D. The sintered specimen composed of grains from 60-100  $\mu\text{m}$  in size. Grains are bound into agglomerates of different sizes and shapes. Fine pores (diameter -20 to 40  $\mu\text{m}$ ) are also present on the grain boundaries.

**La<sub>0.60</sub>Sr<sub>0.40</sub>Co<sub>0.20</sub>Fe<sub>0.80</sub>O<sub>3- $\delta$</sub>  cathode.** The microstructure of a sintered La<sub>0.60</sub>Sr<sub>0.40</sub>Co<sub>0.20</sub>Fe<sub>0.80</sub>O<sub>3- $\delta$</sub>  cathode pellet is shown in Fig. 3E. The average grain sizes are found to 50-100  $\mu\text{m}$  range. All grains are connected with each other leaving small pores. The average pore sizes are found to be in the range of 10 to 35  $\mu\text{m}$ . The large size grains (>10  $\mu\text{m}$ ) present in the sintered body of LSCF specimen may be due to the nucleation of smaller particles at high temperature sintering [24].

**La<sub>0.9</sub>Sr<sub>0.1</sub>Ga<sub>0.8</sub>Mg<sub>0.2</sub>O<sub>3- $\delta$</sub>  electrolyte.** The microstructure of sintered La<sub>0.9</sub>Sr<sub>0.1</sub>Ga<sub>0.8</sub>Mg<sub>0.2</sub>O<sub>3- $\delta$</sub>  specimen is shown in Fig. 3F. From the microstructure, it is clear that the pellet has less pores and uniform grain size distribution. The grain sizes are found to be in the range of 10-25  $\mu\text{m}$ . The pore diameter varied between 5-20  $\mu\text{m}$ . It is also observed that the smaller size (about 10  $\mu\text{m}$ ) grains are connected with larger size grains (about 20  $\mu\text{m}$ ) and leaving little pores.

### Chemical Compatibility between La<sub>0.65</sub>Sr<sub>0.30</sub>MnO<sub>3- $\delta$</sub> Cathode and La<sub>0.9</sub>Sr<sub>0.1</sub>Ga<sub>0.8</sub>Mg<sub>0.2</sub>O<sub>3- $\delta$</sub> electrolyte

**XRD studies.** The X-ray diffraction pattern obtained on 1:1 by wt. of La<sub>0.65</sub>Sr<sub>0.30</sub>MnO<sub>3- $\delta$</sub>  and La<sub>0.9</sub>Sr<sub>0.1</sub>Ga<sub>0.8</sub>Mg<sub>0.2</sub>O<sub>3- $\delta$</sub>  powder mixture calcined at 1573 K for 3 h is shown in Fig. 4A. The comparison of X-ray diffraction data of the individual powders (La<sub>0.65</sub>Sr<sub>0.30</sub>MnO<sub>3- $\delta$</sub>  and La<sub>0.9</sub>Sr<sub>0.1</sub>Ga<sub>0.8</sub>Mg<sub>0.2</sub>O<sub>3- $\delta$</sub> ) and the mixed powder (La<sub>0.65</sub>Sr<sub>0.30</sub>MnO<sub>3- $\delta$</sub>  + La<sub>0.9</sub>Sr<sub>0.1</sub>Ga<sub>0.8</sub>Mg<sub>0.2</sub>O<sub>3- $\delta$</sub> ) is shown in Table 7. It is noted that the La<sub>0.65</sub>Sr<sub>0.30</sub>MnO<sub>3- $\delta$</sub>  calcined with La<sub>0.9</sub>Sr<sub>0.1</sub>Ga<sub>0.8</sub>Mg<sub>0.2</sub>O<sub>3- $\delta$</sub>  at 1573 K for 3 h in air exhibited no reaction products. Also, it is seen that no extra peak corresponding to any other secondary phases are observed. The peaks observed at  $2\theta = 32.4^\circ, 40.1^\circ, 57.9^\circ, 68.2^\circ$  and  $77.6^\circ$  are indexed to both La<sub>0.65</sub>Sr<sub>0.30</sub>MnO<sub>3- $\delta$</sub>  and La<sub>0.9</sub>Sr<sub>0.1</sub>Ga<sub>0.8</sub>Mg<sub>0.2</sub>O<sub>3- $\delta$</sub>  phases since the 'd' values of both the samples are almost same. So, it is drawn that La<sub>0.65</sub>Sr<sub>0.30</sub>MnO<sub>3- $\delta$</sub>  is suitable as cathode with La<sub>0.9</sub>Sr<sub>0.1</sub>Ga<sub>0.8</sub>Mg<sub>0.2</sub>O<sub>3- $\delta$</sub>  based

electrolyte, for ITSOFC.

**SEM studies.** Fig. 4B shows the microstructure of a La<sub>0.65</sub>Sr<sub>0.30</sub>MnO<sub>3- $\delta$</sub>  + La<sub>0.9</sub>Sr<sub>0.1</sub>Ga<sub>0.8</sub>Mg<sub>0.2</sub>O<sub>3- $\delta$</sub>  pellet after sintering at 1573 K for 3 h. The microstructure presented two types of grains (LSGM and LSM) (compare Fig. 3A). However, small pores are also seen in the microstructure. The LSM grains are found to be larger (50  $\mu\text{m}$ ) than the LSGM grains (20  $\mu\text{m}$ ). It is seen that LSGM grains are perfectly linked with LSM grains. The surface of the pellet is smooth. No secondary impurity phases are seen. The pore sizes varied in between 20-50  $\mu\text{m}$ . It is found that the annealing temperature of La<sub>0.65</sub>Sr<sub>0.30</sub>MnO<sub>3- $\delta$</sub>  cathode and La<sub>0.9</sub>Sr<sub>0.1</sub>Ga<sub>0.8</sub>Mg<sub>0.2</sub>O<sub>3- $\delta$</sub>  electrolyte can be maintained at 1573 K during co-firing process for ITSOFC component fabrication.

### Chemical Compatibility between La<sub>0.65</sub>Sr<sub>0.30</sub>FeO<sub>3- $\delta$</sub> cathode and La<sub>0.9</sub>Sr<sub>0.1</sub>Ga<sub>0.8</sub>Mg<sub>0.2</sub>O<sub>3- $\delta$</sub> Electrolyte

**XRD studies.** The X-ray diffraction pattern obtained on 1:1 by wt. of La<sub>0.65</sub>Sr<sub>0.30</sub>FeO<sub>3- $\delta$</sub>  and La<sub>0.9</sub>Sr<sub>0.1</sub>Ga<sub>0.8</sub>Mg<sub>0.2</sub>O<sub>3- $\delta$</sub>  powder mixture calcined at 1573 K for 3 h is shown in Fig. 5A. A comparison of X-ray diffraction data of the individual powder (La<sub>0.65</sub>Sr<sub>0.30</sub>FeO<sub>3- $\delta$</sub>  and La<sub>0.9</sub>Sr<sub>0.1</sub>Ga<sub>0.8</sub>Mg<sub>0.2</sub>O<sub>3- $\delta$</sub> ) and mixed powder (La<sub>0.65</sub>Sr<sub>0.30</sub>FeO<sub>3- $\delta$</sub>  + La<sub>0.9</sub>Sr<sub>0.1</sub>Ga<sub>0.8</sub>Mg<sub>0.2</sub>O<sub>3- $\delta$</sub> ) has been made in Table 8. It is reported that the La<sub>0.80</sub>Sr<sub>0.20</sub>FeO<sub>3- $\delta$</sub>  cathode showed no reaction with YSZ [25]. Similarly, it has been reported that there is no reaction products between La<sub>0.70</sub>Sr<sub>0.20</sub>FeO<sub>3- $\delta$</sub>  and YSZ upto 1273 K, while at 1373 K, Sr<sub>2</sub>ZrO<sub>4</sub> as a reaction product was observed [26]. No report is available on the chemical compatibility of La<sub>0.65</sub>Sr<sub>0.30</sub>FeO<sub>3- $\delta$</sub>  cathode and La<sub>0.9</sub>Sr<sub>0.1</sub>Ga<sub>0.8</sub>Mg<sub>0.2</sub>O<sub>3- $\delta$</sub>  electrolyte. From the data given in Table 8, it is noted that La<sub>0.65</sub>Sr<sub>0.30</sub>FeO<sub>3- $\delta$</sub>  calcined with La<sub>0.9</sub>Sr<sub>0.1</sub>Ga<sub>0.8</sub>Mg<sub>0.2</sub>O<sub>3- $\delta$</sub>  at 1573 K for 3 h exhibited no reaction products. Secondary phases between La<sub>0.65</sub>Sr<sub>0.30</sub>FeO<sub>3- $\delta$</sub>  and La<sub>0.9</sub>Sr<sub>0.1</sub>Ga<sub>0.8</sub>Mg<sub>0.2</sub>O<sub>3- $\delta$</sub>  could not be observed in the XRD pattern. The peaks observed at  $2\theta = 32.2^\circ, 39.8^\circ, 46.3^\circ, 57.5^\circ, 67.6^\circ, \text{ and } 77.0^\circ$  are indexed to both La<sub>0.65</sub>Sr<sub>0.30</sub>FeO<sub>3- $\delta$</sub>  and La<sub>0.9</sub>Sr<sub>0.1</sub>Ga<sub>0.8</sub>Mg<sub>0.2</sub>O<sub>3- $\delta$</sub>  phases, since the 'd' values of both the samples are similar. From the chemical compatibility experiment, it was observed that La<sub>0.65</sub>Sr<sub>0.30</sub>FeO<sub>3- $\delta$</sub>  cathode did not react and exhibited good compatibility with La<sub>0.9</sub>Sr<sub>0.1</sub>Ga<sub>0.8</sub>Mg<sub>0.2</sub>O<sub>3- $\delta$</sub>  electrolyte. Thus, this LSF-LSGM9182 combination can be used in the co-firing process for ITSOFC application.

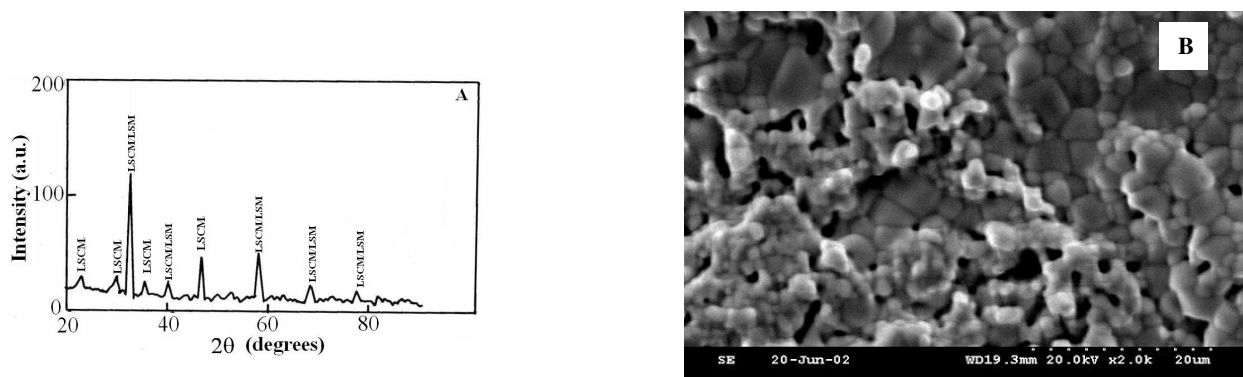


**Fig. 4.** (A) Powder XRD pattern obtained on  $\text{La}_{0.65}\text{Sr}_{0.30}\text{MnO}_{3-\delta}$  and  $\text{La}_{0.9}\text{Sr}_{0.1}\text{Ga}_{0.8}\text{Mg}_{0.2}\text{O}_{3-\delta}$  1:1 (by wt.) mixture calcined at 1573 K for 3 h and (B) SEM photograph obtained on  $\text{La}_{0.65}\text{Sr}_{0.30}\text{MnO}_{3-\delta}$  +  $\text{La}_{0.9}\text{Sr}_{0.1}\text{Ga}_{0.8}\text{Mg}_{0.2}\text{O}_{3-\delta}$  pellet after sintering at 1573 K for 3 h.

**Table 7.** Comparison of XRD Data of Individual Powders with the XRD Data of  $\text{La}_{0.65}\text{Sr}_{0.30}\text{MnO}_{3-\delta}$  +  $\text{La}_{0.9}\text{Sr}_{0.1}\text{Ga}_{0.8}\text{Mg}_{0.2}\text{O}_{3-\delta}$  Powder Mixture after Annealing at 1573 K for 3 h

XRD data for LSM + LSGM9182 powder mixture			XRD data for LSM			XRD data for LSGM9182	
Peak No.	2θ values	d values	Peak assigned for	2θ values	d values	2θ values	d values
1	22.800	3.897	LSGM	-	-	22.700	3.9141
2	29.800	2.996	LSGM	-	-	30.100	2.9660
3	32.400	2.761	LSGM/LSM	33.000	2.712	32.600	2.7445
4	35.400	2.534	LSGM	-	-	34.800	2.5760
5	40.100	2.247	LSGM/LSM	40.700	2.215	40.000	2.2522
6	46.600	1.947	LSM	-	-	46.700	1.9435
7	57.900	1.591	LSGM/LSM	58.700	1.572	58.000	1.5889
8	68.200	1.374	LSGM/LSM	68.900	1.362	68.000	1.3775
9	77.600	1.229	LSGM/LSM	78.300	1.220	77.500	1.2307

**SEM studies.** Figure 5B shows the microstructure of a  $\text{La}_{0.65}\text{Sr}_{0.30}\text{FeO}_{3-\delta}$  +  $\text{La}_{0.9}\text{Sr}_{0.1}\text{Ga}_{0.8}\text{Mg}_{0.2}\text{O}_{3-\delta}$  pellet after sintering at 1573 K for 3 h. Two types of grains are observed. One group of grains are found to be larger than the other. The larger grains are assigned to LSF particles (Fig. 3B) in the range of 100 μm in size that may be due to the agglomeration of particles at high temperatures. The LSF grains are found to be strongly linked with each other. In some places, LSGM grains are also attached with the LSF grains. The micrograph

exhibits porosity with a pore size of 50 μm. No other secondary phases are seen which is in consistency with the XRD results. SEM and XRD observations indicated that the LSF cathode is a choice for the LSGM based ITSOFC.

#### **Chemical Compatibility between $\text{La}_{0.70}\text{Sr}_{0.30}\text{CoO}_{3-\delta}$ Cathode and $\text{La}_{0.9}\text{Sr}_{0.1}\text{Ga}_{0.8}\text{Mg}_{0.2}\text{O}_{3-\delta}$ Electrolyte**

**XRD studies.** The X-ray diffraction pattern obtained on of  $\text{La}_{0.70}\text{Sr}_{0.30}\text{CoO}_{3-\delta}$  and  $\text{La}_{0.9}\text{Sr}_{0.1}\text{Ga}_{0.8}\text{Mg}_{0.2}\text{O}_{3-\delta}$  1:1 (by wt.)

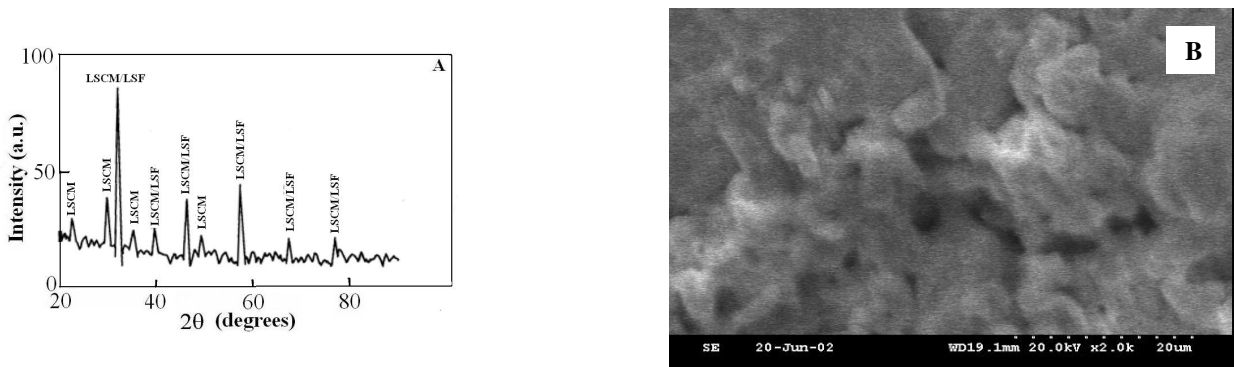


**Fig. 5.** (A) Powder XRD pattern obtained on  $\text{La}_{0.65}\text{Sr}_{0.30}\text{FeO}_{3-\delta}$  and  $\text{La}_{0.9}\text{Sr}_{0.1}\text{Ga}_{0.8}\text{Mg}_{0.2}\text{O}_{3-\delta}$  1:1 (by wt.) mixture calcined at 1573 K for 3 h and (B) SEM photograph obtained on  $\text{La}_{0.65}\text{Sr}_{0.30}\text{FeO}_{3-\delta}$  +  $\text{La}_{0.9}\text{Sr}_{0.1}\text{Ga}_{0.8}\text{Mg}_{0.2}\text{O}_{3-\delta}$  pellet after sintering at 1573 K for 3 h.

**Table 8.** Comparison of XRD Data of Individual Powders with the XRD Data of  $\text{La}_{0.65}\text{Sr}_{0.30}\text{FeO}_{3-\delta}$  +  $\text{La}_{0.9}\text{Sr}_{0.1}\text{Ga}_{0.8}\text{Mg}_{0.2}\text{O}_{3-\delta}$  Powder Mixture after Annealing at 1573 K for 3 h

XRD data for LSF + LSGM9182 powder mixture			XRD data for LSF			XRD data for LSGM9182	
Peak No.	2θ values	d values	Peak assigned for	2θ values	d values	2θ values	d values
1	22.600	3.931	LSGM	-	-	22.700	3.9141
2	29.800	2.996	LSGM	-	-	30.100	2.9660
3	32.200	2.778	LSGM/LSF	32.700	2.736	32.600	2.7445
4	35.200	2.547	LSGM	-	-	34.800	2.5760
5	39.800	2.263	LSGM/LSF	40.200	2.241	40.000	2.2522
6	46.300	1.959	LSGM/LSF	46.800	1.940	46.700	1.9435
7	49.400	1.843	LSGM	-	-	49.600	1.8364
8	57.500	1.601	LSGM/LSF	58.000	1.589	58.000	1.5889
9	67.600	1.385	LSGM/LSF	68.200	1.374	68.000	1.3775
10	77.000	1.237	LSGM/LSF	77.600	1.229	77.500	1.2307

powder mixture calcined at 1573 K for 3 h is shown in Fig. 6A. Comparison of X-ray diffraction data of the individual powder ( $\text{La}_{0.70}\text{Sr}_{0.30}\text{CoO}_{3-\delta}$  and  $\text{La}_{0.9}\text{Sr}_{0.1}\text{Ga}_{0.8}\text{Mg}_{0.2}\text{O}_{3-\delta}$ ) and their mixed powder ( $\text{La}_{0.70}\text{Sr}_{0.30}\text{CoO}_{3-\delta}$  +  $\text{La}_{0.9}\text{Sr}_{0.1}\text{Ga}_{0.8}\text{Mg}_{0.2}\text{O}_{3-\delta}$ ) are shown in Table 9.  $\text{La}_{1-x}\text{Sr}_x\text{CoO}_{3-\delta}$  is considered as a cathode for SOFCs because of its high electronic conductivity and high catalytic activity. However, it

is reported that LSC reacts with YSZ electrolyte at high temperatures to form  $\text{La}_2\text{Zr}_2\text{O}_7$  or  $\text{SrZrO}_3$  [26-27]. Thus, LSC is not a suitable cathode for the YSZ electrolyte in SOFCs. Ishihara *et al.* reported that new secondary phases between  $\text{La}_{0.9}\text{Sr}_{0.1}\text{Ga}_{0.8}\text{Mg}_{0.2}\text{O}_{3-\delta}$  and  $\text{La}_{0.60}\text{Sr}_{0.40}\text{CoO}_{3-\delta}$  could not be observed in XRD pattern below 1473 K, when a mixture of the same weight of each powder was calcined [15]. Huang *et al.*

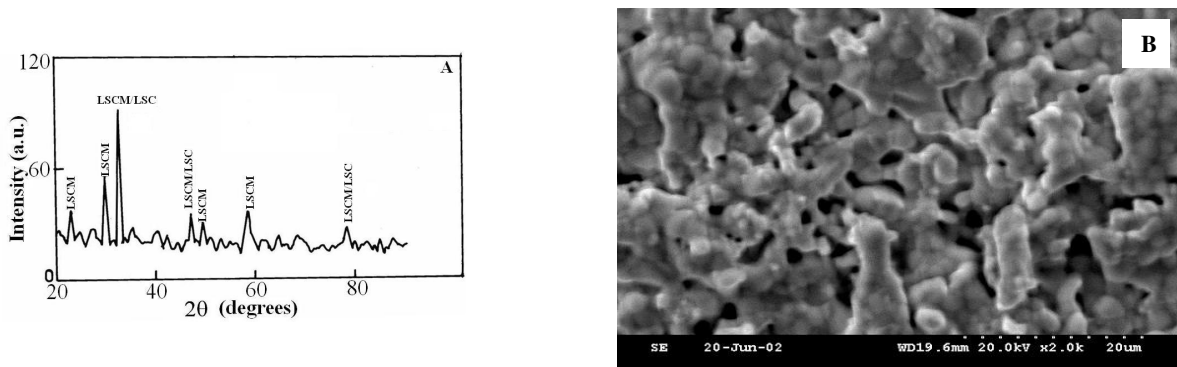


**Fig. 6.** (A) Powder XRD pattern obtained on of  $\text{La}_{0.70}\text{Sr}_{0.30}\text{CoO}_{3-\delta}$  and  $\text{La}_{0.9}\text{Sr}_{0.1}\text{Ga}_{0.8}\text{Mg}_{0.2}\text{O}_{3-\delta}$  1:1 (by wt.) mixture calcined at 1573 K for 3 h and (B) SEM photograph obtained on pellet after sintering at 1573 K for 3 h.

**Table 9.** Comparison of XRD Data of Individual Powders with the XRD Data of  $\text{La}_{0.70}\text{Sr}_{0.30}\text{CoO}_{3-\delta}$  +  $\text{La}_{0.9}\text{Sr}_{0.1}\text{Ga}_{0.8}\text{Mg}_{0.2}\text{O}_{3-\delta}$  Powder Mixture after Annealing at 1573 K for 3 h

XRD data for LSC + LSGM9182 powder mixture			XRD data for LSC		XRD data for LSGM9182		
Peak No.	2θ values	d values	Peak assigned for	2θ values	d values	2θ values	d values
1	22.800	3.897	LSGM	-	-	22.700	3.9141
2	29.800	2.996	LSGM	-	-	30.100	2.9660
3	32.700	2.736	LSGM/LSC	33.400	2.681	32.600	2.7445
4	47.000	1.932	LSGM/LSC	47.800	1.901	46.700	1.9435
5	49.400	1.843	LSGM	-	-	49.600	1.8364
6	58.400	1.579	LSGM	-	-	58.000	1.5889
7	78.400	1.219	LSGM/LSC	79.500	1.205	68.000	1.3775

investigated the chemical reaction between  $\text{La}_{0.50}\text{Sr}_{0.50}\text{CoO}_{3-\delta}$  and  $\text{La}_{0.9}\text{Sr}_{0.1}\text{Ga}_{0.8}\text{Mg}_{0.2}\text{O}_{3-\delta}$ . They reported interdiffusion of B site cations (Co in LSC and Ga in LSGM) at 1323 K in 2 h [28]. However, LSC cathodes showed high performance on doped  $\text{LaGaO}_3$  electrolytes at a temperature range of 873-1073 K [29-30]. Reports on the long-term stability at the LSC/LSGM interface are scarce [31]. From the data given in Table 9, it is noted that the  $\text{La}_{0.70}\text{Sr}_{0.30}\text{CoO}_{3-\delta}$  and  $\text{La}_{0.9}\text{Sr}_{0.1}\text{Ga}_{0.8}\text{Mg}_{0.2}\text{O}_{3-\delta}$  at 1573 K for 3 h exhibit no reaction products. Also, it is seen that the peaks observed at  $2\theta = 32.7^\circ$ ,  $47.0^\circ$  and  $78.4^\circ$  are indexed to both  $\text{La}_{0.70}\text{Sr}_{0.30}\text{CoO}_{3-\delta}$  and  $\text{La}_{0.9}\text{Sr}_{0.1}\text{Ga}_{0.8}\text{Mg}_{0.2}\text{O}_{3-\delta}$  phases since the 'd' values of both the

samples are similar.

**SEM studies.** Figure 6B shows the microstructure of a  $\text{La}_{0.70}\text{Sr}_{0.30}\text{CoO}_{3-\delta}$  +  $\text{La}_{0.9}\text{Sr}_{0.1}\text{Ga}_{0.8}\text{Mg}_{0.2}\text{O}_{3-\delta}$  pellet after sintering at 1573 K for 3 h. The microstructure showed that the sintered specimen composed of two grains (LSC and LSGM) (compare Fig. 3C). Mostly, all LSGM particles are well linked with each other. The grains are not uniform. The LSGM grains are 50  $\mu\text{m}$  in size and the LSC grains are 20  $\mu\text{m}$  in size. The pore size is 20  $\mu\text{m}$ . No other new phases are observed. The LSC + LSGM pellet attained 40% densification after sintering at 1573 K for 3 h which indicates the porous nature of the sample. The presence of pores is evident from the

surface microstructure. From the XRD and SEM studies, it was found that the  $\text{La}_{0.70}\text{Sr}_{0.30}\text{CoO}_{3-\delta}$  cathode and  $\text{La}_{0.9}\text{Sr}_{0.1}\text{Ga}_{0.8}\text{Mg}_{0.2}\text{O}_{3-\delta}$  electrolyte can be annealed at 1573 K during co-firing process for application in ITSOFC.

### Chemical Compatibility between $\text{La}_{0.65}\text{Sr}_{0.30}\text{NiO}_{3-\delta}$ Cathode and $\text{La}_{0.9}\text{Sr}_{0.1}\text{Ga}_{0.8}\text{Mg}_{0.2}\text{O}_{3-\delta}$ Electrolyte

**XRD studies.** The X-ray diffraction pattern obtained on a  $\text{La}_{0.65}\text{Sr}_{0.30}\text{NiO}_{3-\delta}$  and  $\text{La}_{0.9}\text{Sr}_{0.1}\text{Ga}_{0.8}\text{Mg}_{0.2}\text{O}_{3-\delta}$  1:1 (by wt.) powder mixture calcined at 1573 K for 3 h is shown in Fig. 7A. A comparison of X-ray diffraction data of the individual powders ( $\text{La}_{0.65}\text{Sr}_{0.30}\text{NiO}_{3-\delta}$  and  $\text{La}_{0.9}\text{Sr}_{0.1}\text{Ga}_{0.8}\text{Mg}_{0.2}\text{O}_{3-\delta}$ ) and mixed powder ( $\text{La}_{0.65}\text{Sr}_{0.30}\text{NiO}_{3-\delta}$  +  $\text{La}_{0.9}\text{Sr}_{0.1}\text{Ga}_{0.8}\text{Mg}_{0.2}\text{O}_{3-\delta}$ ) has been made in Table 10. It is reported that  $\text{LaNiO}_3$  reacts with the YSZ electrolyte at high temperature (1473 K) to form  $\text{La}_2\text{Zr}_2\text{O}_7$ ,  $\text{La}_2\text{NiO}_4$  and  $\text{NiO}$  [22]. No report is available on the chemical compatibility of  $\text{La}_{0.9}\text{Sr}_{0.1}\text{Ga}_{0.8}\text{Mg}_{0.2}\text{O}_{3-\delta}$  with  $\text{La}_{0.65}\text{Sr}_{0.30}\text{NiO}_{3-\delta}$  cathode. It has also been reported that the SOFC exhibits low performance when the anodes are fabricated from NiO-LSGM cermet in contact with LSGM electrolyte, because of the interdiffusion and reaction at the interface [32]. From Table 10 and Fig. 7A, it is seen that the  $\text{La}_{0.65}\text{Sr}_{0.30}\text{NiO}_{3-\delta}$  calcined with  $\text{La}_{0.9}\text{Sr}_{0.1}\text{Ga}_{0.8}\text{Mg}_{0.2}\text{O}_{3-\delta}$  at 1573 K for 3 h exhibited two new peaks in the XRD pattern at  $2\theta = 27.7^\circ$  and  $31.3^\circ$ , which are due to the formation of new phases. However, it was very difficult to confirm the identity of the material because of its very low intensity. It is reported that above 1173 K,  $\text{LaNiO}_3$  decomposes to several La-Ni-O oxides [33]. It is seen that the peaks observed at  $2\theta = 32.5^\circ$ ,  $46.7^\circ$  and  $58.0^\circ$  are indexed to both  $\text{La}_{0.65}\text{Sr}_{0.30}\text{NiO}_{3-\delta}$  and  $\text{La}_{0.9}\text{Sr}_{0.1}\text{Ga}_{0.8}\text{Mg}_{0.2}\text{O}_{3-\delta}$  phases, since the 'd' values of both the samples are found to be similar. Also, it is found that the new phases formed [34] may be due to the decomposition of  $\text{La}_{0.65}\text{Sr}_{0.30}\text{NiO}_{3-\delta}$  at high temperature i.e., 1573 K for 3 h. These results confirm prior results that Ni reacts with LSGM to form insulating phases at elevated temperatures [35]. Due to the formation of new phases after high temperature treatment (1573 K for 3 h), it is drawn that  $\text{La}_{0.65}\text{Sr}_{0.30}\text{NiO}_{3-\delta}$  may not be a suitable cathode for the  $\text{La}_{0.9}\text{Sr}_{0.1}\text{Ga}_{0.8}\text{Mg}_{0.2}\text{O}_{3-\delta}$  electrolyte in ITSOFC.

**SEM studies.** Figure 7B shows the microstructure of a  $\text{La}_{0.65}\text{Sr}_{0.30}\text{NiO}_{3-\delta}$  +  $\text{La}_{0.9}\text{Sr}_{0.1}\text{Ga}_{0.8}\text{Mg}_{0.2}\text{O}_{3-\delta}$  pellet after sintering at 1573 K for 3 h. The microstructure shows two

types of grains (compare Fig. 3D) namely, LSN and LSGM along with impurity phases. The LSGM grains are connected with each other leaving some pores. LSN grains are seen in between LSGM grains. The pore size is 40  $\mu\text{m}$ . The sizes for LSGM and LSN grains are 30 and 40  $\mu\text{m}$ , respectively. From the above investigations, it is concluded that the heat treatment of  $\text{La}_{0.65}\text{Sr}_{0.30}\text{NiO}_{3-\delta}$  cathode with  $\text{La}_{0.9}\text{Sr}_{0.1}\text{Ga}_{0.8}\text{Mg}_{0.2}\text{O}_{3-\delta}$  electrolyte at 1573 K for 3 h produce new phases and  $\text{La}_{0.65}\text{Sr}_{0.30}\text{NiO}_{3-\delta}$  cannot be considered as a cathode for  $\text{La}_{0.9}\text{Sr}_{0.1}\text{Ga}_{0.8}\text{Mg}_{0.2}\text{O}_{3-\delta}$  electrolyte in ITSOFC.

### Chemical Compatibility between $\text{La}_{0.60}\text{Sr}_{0.40}\text{Co}_{0.20}\text{Fe}_{0.80}\text{O}_{3-\delta}$ Cathode and $\text{La}_{0.9}\text{Sr}_{0.1}\text{Ga}_{0.8}\text{Mg}_{0.2}\text{O}_{3-\delta}$ Electrolyte

**XRD studies.** The X-ray diffraction pattern obtained on a  $\text{La}_{0.60}\text{Sr}_{0.40}\text{Co}_{0.20}\text{Fe}_{0.80}\text{O}_{3-\delta}$  and  $\text{La}_{0.9}\text{Sr}_{0.1}\text{Ga}_{0.8}\text{Mg}_{0.2}\text{O}_{3-\delta}$  1:1 (by wt.) powder mixture calcined at 1573 K for 3 h is shown in Fig. 8A. A comparison of X-ray diffraction data of the individual powder ( $\text{La}_{0.60}\text{Sr}_{0.40}\text{Co}_{0.20}\text{Fe}_{0.80}\text{O}_{3-\delta}$  and  $\text{La}_{0.9}\text{Sr}_{0.1}\text{Ga}_{0.8}\text{Mg}_{0.2}\text{O}_{3-\delta}$ ) and their mixed powders ( $\text{La}_{0.60}\text{Sr}_{0.40}\text{Co}_{0.20}\text{Fe}_{0.80}\text{O}_{3-\delta}$  +  $\text{La}_{0.9}\text{Sr}_{0.1}\text{Ga}_{0.8}\text{Mg}_{0.2}\text{O}_{3-\delta}$ ) has been made in Table 11. It is reported that  $\text{La}_{0.60}\text{Sr}_{0.40}\text{Co}_{0.20}\text{Fe}_{0.80}\text{O}_{3-\delta}$  reacts with YSZ electrolyte at 1273 K in 1300 h to form  $\text{SrZrO}_3$  perovskite and  $\text{La}_2\text{Zr}_2\text{O}_7$  pyrochlore [36], whereas no details are available on the chemical compatibility of LSCF with LSGM electrolytes. But, it is reported that best oxygen permeability exists for the LSGM/LSCF combination, processed under moderate firing conditions [37]. From Table 11 and Fig. 8A, it is noted that the  $\text{La}_{0.60}\text{Sr}_{0.40}\text{Co}_{0.20}\text{Fe}_{0.80}\text{O}_{3-\delta}$  calcined with  $\text{La}_{0.9}\text{Sr}_{0.1}\text{Ga}_{0.8}\text{Mg}_{0.2}\text{O}_{3-\delta}$  at 1573 K for 3 h exhibits a new peak at  $2\theta = 27.6^\circ$  owing to the formation of an impurity phase. Also, it is seen that the peaks observed at  $2\theta = 32.4^\circ$ ,  $57.8^\circ$ , and  $67.8^\circ$  are indexed to both  $\text{La}_{0.60}\text{Sr}_{0.40}\text{Co}_{0.20}\text{Fe}_{0.80}\text{O}_{3-\delta}$  and  $\text{La}_{0.9}\text{Sr}_{0.1}\text{Ga}_{0.8}\text{Mg}_{0.2}\text{O}_{3-\delta}$  phases since the 'd' values of both the samples are similar. Thus,  $\text{La}_{0.60}\text{Sr}_{0.40}\text{Co}_{0.20}\text{Fe}_{0.80}\text{O}_{3-\delta}$  may not be a suitable candidate cathode for  $\text{La}_{0.9}\text{Sr}_{0.1}\text{Ga}_{0.8}\text{Mg}_{0.2}\text{O}_{3-\delta}$  electrolyte for high temperature co-firing process in ITSOFC.

**SEM studies.** Figure 8B shows the microstructure of  $\text{La}_{0.60}\text{Sr}_{0.40}\text{Co}_{0.20}\text{Fe}_{0.80}\text{O}_{3-\delta}$  +  $\text{La}_{0.9}\text{Sr}_{0.1}\text{Ga}_{0.8}\text{Mg}_{0.2}\text{O}_{3-\delta}$  pellet sintered at 1573 K for 3 h. From Fig. 8B, it is seen that the surface morphology of the pellet is not uniform. Also, it is observed that the LSGM grains completely covered the LSCF

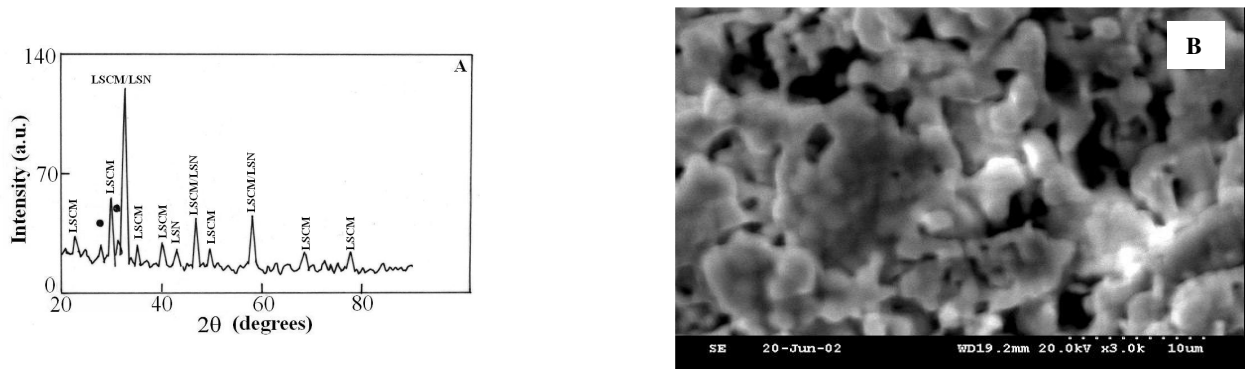


**Fig. 7.** (A) Powder XRD pattern obtained on of  $\text{La}_{0.65}\text{Sr}_{0.30}\text{NiO}_{3-\delta}$  and  $\text{La}_{0.9}\text{Sr}_{0.1}\text{Ga}_{0.8}\text{Mg}_{0.2}\text{O}_{3-\delta}$  1:1 (by wt.) mixture calcined at 1573 K for 3 h and (B) SEM photograph obtained on  $\text{La}_{0.65}\text{Sr}_{0.30}\text{NiO}_{3-\delta}$  +  $\text{La}_{0.9}\text{Sr}_{0.1}\text{Ga}_{0.8}\text{Mg}_{0.2}\text{O}_{3-\delta}$  pellet after sintering at 1573 K for 3 h.

**Table 10.** Comparison of XRD Data of Individual Powders with the XRD Data of  $\text{La}_{0.65}\text{Sr}_{0.30}\text{NiO}_{3-\delta}$  +  $\text{La}_{0.9}\text{Sr}_{0.1}\text{Ga}_{0.8}\text{Mg}_{0.2}\text{O}_{3-\delta}$  Powder Mixture after Annealing at 1573 K for 3 h

XRD data for LSN + LSGM9182 powder mixture			XRD data for LSN			XRD data for LSGM9182	
Peak No.	2θ values	d values	Peak assigned for	2θ values	d values	2θ values	d values
1	22.600	3.931	LSGM	-	-	22.700	3.9141
2	22.700	3.218	IMPURITY	-	-	-	-
3	29.800	2.996	LSGM	-	-	30.100	2.9660
4	31.300	2.855	IMPURITY	-	-	-	-
5	32.500	2.753	LSGM/LSN	33.100	2.704	32.600	2.7445
6	35.200	2.547	LSGM	-	-	34.800	2.5760
7	40.000	2.252	LSGM	-	-	40.000	2.2522
8	42.800	2.111	LSN	43.600	2.074	-	-
9	46.700	1.943	LSGM/LSN	47.600	1.909	46.700	1.9435
10	49.400	1.843	LSGM	-	-	49.600	1.8364
11	58.000	1.589	LSGM/LSN	58.000	1.569	58.000	1.5889
12	68.300	1.372	LSGM	-	-	68.000	1.3775
13	77.000	1.228	LSGM	-	-	77.500	1.2307

grains (compare Fig. 3E). Also, it is seen that the sintering of LSGM + LSCF particles resulted in the formation of large agglomerates of size upto 100  $\mu\text{m}$ . The pore sizes varied between 30-50  $\mu\text{m}$ . From the above investigations, it can be concluded that  $\text{La}_{0.60}\text{Sr}_{0.40}\text{Co}_{0.20}\text{Fe}_{0.80}\text{O}_{3-\delta}$  cathode may not be a

choice for  $\text{La}_{0.9}\text{Sr}_{0.1}\text{Ga}_{0.8}\text{Mg}_{0.2}\text{O}_{3-\delta}$  electrolyte in ITSOFC.

## CONCLUSIONS

The main issue concerning the appropriate cathode and

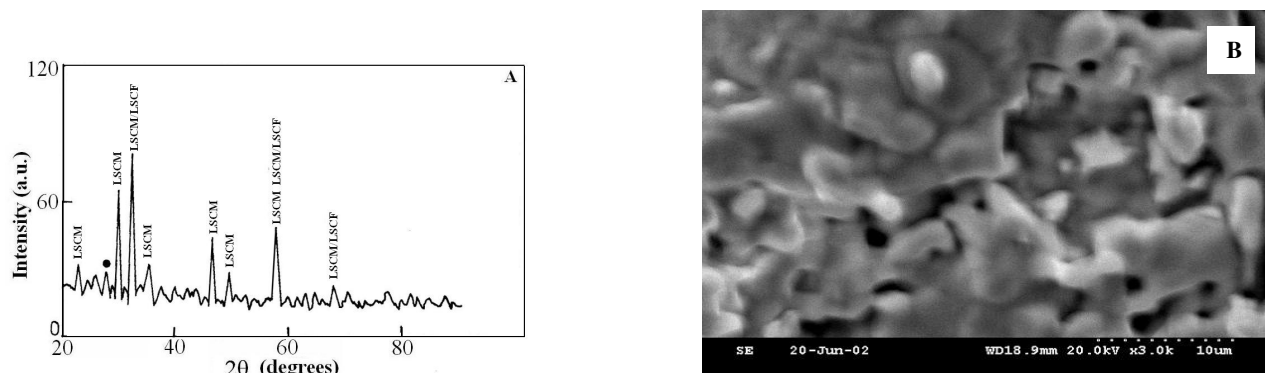


**Fig. 8.** (A) Powder XRD pattern obtained on of  $\text{La}_{0.60}\text{Sr}_{0.40}\text{Co}_{0.20}\text{Fe}_{0.80}\text{O}_{3-\delta}$  and  $\text{La}_{0.9}\text{Sr}_{0.1}\text{Ga}_{0.8}\text{Mg}_{0.2}\text{O}_{3-\delta}$  1:1 (by wt.) mixture calcined at 1573 K for 3 h and (B) SEM photograph obtained on  $\text{La}_{0.60}\text{Sr}_{0.40}\text{Co}_{0.20}\text{Fe}_{0.80}\text{O}_{3-\delta}$  +  $\text{La}_{0.9}\text{Sr}_{0.1}\text{Ga}_{0.8}\text{Mg}_{0.2}\text{O}_{3-\delta}$  pellet after sintering at 1573 K for 3 h.

**Table 11.** Comparison of XRD Data of Individual Powders with the XRD Data of  $\text{La}_{0.60}\text{Sr}_{0.40}\text{Co}_{0.20}\text{Fe}_{0.80}\text{O}_{3-\delta}$  +  $\text{La}_{0.9}\text{Sr}_{0.1}\text{Ga}_{0.8}\text{Mg}_{0.2}\text{O}_{3-\delta}$  Powder Mixture after Annealing at 1573 K for 3 h

XRD data for LSCF + LSGM9182 powder mixture			XRD data for LSCF		XRD data for LSGM9182		
Peak No.	2θ values	d values	Peak assigned for	2θ values	d values	2θ values	d values
1	22.600	3.931	LSGM	-	-	22.700	3.9141
2	27.600	3.229	IMPURITY	-	-	-	-
3	29.800	2.996	LSGM	-	-	30.100	2.9660
4	32.400	2.761	LSGM/LSCF	33.000	2.712	32.600	2.7445
5	35.400	2.534	LSGM	-	-	34.800	2.5760
6	46.500	1.951	LSGM	-	-	46.700	1.9435
7	49.500	1.840	LSGM	-	-	49.600	1.8364
8	57.800	1.594	LSGM/LSCF	58.600	1.574	58.000	1.5889
9	67.800	1.381	LSGM/LSCF	68.900	1.362	68.000	1.3775

electrolyte materials for ITSOFC application is the formation of new interfacial phases, which are detrimental for the conductivity in the boundary. From the reactivity experiments between cathodes and alternate electrolytes, the following conclusions are drawn.

1. The  $\text{La}_{0.65}\text{Sr}_{0.30}\text{MnO}_{3-\delta}$ ,  $\text{La}_{0.65}\text{Sr}_{0.30}\text{FeO}_{3-\delta}$  and  $\text{La}_{0.70}\text{Sr}_{0.30}\text{CoO}_{3-\delta}$  cathodes showed no reaction product

when mixed and calcined with  $\text{La}_{0.9}\text{Sr}_{0.1}\text{Ga}_{0.8}\text{Mg}_{0.2}\text{O}_{3-\delta}$  electrolyte. Thus, these three cathodes are useful with LSGM electrolyte in ITSOFC.

2. The  $\text{La}_{0.65}\text{Sr}_{0.30}\text{NiO}_{3-\delta}$  and  $\text{La}_{0.60}\text{Sr}_{0.40}\text{Co}_{0.20}\text{Fe}_{0.80}\text{O}_{3-\delta}$  cathodes reacted with  $\text{La}_{0.9}\text{Sr}_{0.1}\text{Ga}_{0.8}\text{Mg}_{0.2}\text{O}_{3-\delta}$  electrolyte and showed new reaction products. Hence, these two cathodes may not be useful with LSGM electrolyte in ITSOFC.

## ACKNOWLEDGEMENTS

A.S. Nesaraj thanks Council of Scientific and Industrial Research, Government of India for awarding him Senior Research Fellowship to carry out his Ph.D. research work in Fuel Cells Laboratory, Central Electrochemical Research Institute, Karaikudi, India. He also thanks the management of Karunya University, Coimbatore, India for its encouragement and interest in this research activity.

## REFERENCES

- [1] T. Fukui, S. Ohara, K. Murata, H. Yoshida, K. Miura, T. Inagaki, *J. Power Sources* 106 (2002) 142.
- [2] R.N. Basu, S.K. Pratihar, M. Saha, H.S. Maiti, *Mater. Lett.* 32 (1997) 217.
- [3] C.Ch. Kostogloudis, Ch. Ftikos, *J. Euro. Ceram. Soc.* 19 (1999) 497.
- [4] T. Inagaki, K. Miura, H. Yoshida, R. Maric, S. Ohara, X. Zhang, K. Mukai, T. Fukui, *J. Power Sources* 86 (2000) 347.
- [5] J.P.P. Huijsmans, F.P.F. van Berkel, G.M. Christie, *J. Power Sources* 71 (1998) 107.
- [6] T. Ishihara, H. Matsuda, Y. Takita, *J. Am. Ceram. Soc.* 116 (1994) 3801.
- [7] K. Wiik, C.R. Schmidt, S. Faaland, S. Shamsili, M.-A. Einarsrud, T. Grande, *J. Am. Ceram. Soc.* 82 (1999) 721.
- [8] G. Stochniol, S. Broelo, A. Naoumidis, H. Nickel, *Fresenius J. Anal. Chem.* 355 (1996) 697.
- [9] T. Kawada, N. Sakai, H. Yokokawa, M. Dokiya, *Solid State Ionics* 50 (1992) 189.
- [10] B. Gharbage, T. Pagnier, A. Hammou, *J. Electrochem. Soc.* 141 (1994) 2118.
- [11] Y. Ohno, S. Nagata, H. Sato, *Solid State Ionics* 9/10 (1983) 1001.
- [12] A. Tsoga, A. Gupta, A. Naoumidis, P. Nikolopoulos, *Acta Mater.* 48 (2000) 4709.
- [13] G. Stochniol, E. Syskakis, A. Naoumidis, SOFC, Materials, Process Engineering and Electrochemistry, 5<sup>th</sup> IEA Workshop Julich, Germany, 2-4 March 1993, pp. 25-31.
- [14] A. Samson Nesaraj, Studies on materials and components for Intermediate Temperature Solid Oxide Fuel Cells Ph.D. Thesis, Alagappa University, India, 2002.
- [15] P. Huang, A. Petric, *J. Electrochem. Soc.* 143 (1996) 1644.
- [16] M. Rozumek, P. Majewski, L. Sauter, F. Aldinger, *J. Am. Ceram. Soc.* 86 (2003) 1940.
- [17] T. Mimani, *Resonance* 5 (2000) 50.
- [18] R.D. Purohit, A.K. Tyagi, M.D. Mathews, S. Saha, *J. Nuclear Mater.* 280 (2000) 50.
- [19] N. Arul Dhas, K.C. Patil, *J. Mater. Sci. Lett.* 12 (1993) 1844.
- [20] L. El. Frah, M. Massor, M. Lemal, C. Julien, S. Chitra, P. Kalyan, T. Mohan, R. Gangadharan, *J. Electroceram.* 3-4 (1999) 425.
- [21] B.C.H. Steele, *J. Power Sources* 49 (1994) 1.
- [22] K. Wiik, C.R. Schmidt, S. Faaland, S. Shamsili, M.-A. Einarsrud, T. Grande, *J. Am. Ceram. Soc.* 82 (1999) 721.
- [23] V.V. Kharton, F.M. Figueiredo, A.V. Kovalevsky, A.P. Viskup, E.N. Naumovich, A.A. Yaremchenko, I.A. Boshmakov, F.M.B. Marques, *J. Euro. Ceram. Soc.* 21 (2001) 2301.
- [24] S. Shi, J.-Y. Hwang, *J. Min. & Mat. Character. & Eng.* 2 (2003) 145.
- [25] J.M. Ralph, A. Schoeler, M. Krumpelt, *J. Mat. Sci.* 36 (2001) 1162.
- [26] O. Yamamoto, Y. Takeda, R. Kanno, M. Noda, *Solid State Ionics* 22 (1987) 241.
- [27] N.Q. Minh, *J. Am. Ceram. Soc.* 76 (1993) 563.
- [28] K. Huang, M. Feng, J.B. Goodenough, M. Schmerling, *J. Electrochem. Soc.* 143 (1996) 3630.
- [29] K. Huang, R. Tichy, J.B. Goodenough, *J. Am Ceram Soc.* 81 (1998) 2581.
- [30] T. Ishihara, H. Minami, H. Matsuda, H. Nishiguchi, Y. Takita, *Chem. Commun.* (1996) 929.
- [31] R. Maric, S. Ohara, R. Maric, T. Fukui, H. Yoshida, T. Inagaki, K. Miura, in: S.C. Singhal, M. Dokiya (Eds.), Proc. Sixth International Symposium on Solid Oxide Fuel Cells (SOFC-VI), NJ, 1999.
- [32] P. Huang, A. Horky, A. Petric, *J. Am. Ceram. Soc.* 82 (1999) 2402.
- [33] M.T. Colomer, A. Martinez, P. Recio, C. Pascual, J.R.

- Jurado, in: P. Stevens (Ed.), Proc. Symposium European Solid Oxide Fuel Cells, Nantes, 1998.
- [34] H. Seim, H. Mölsa, M. Nieminen, L. Niinistö, H. Fjellvåg, *J. Mater. Chem.* 7 (1997) 449.
- M. Feng, J.B. Goodenough, K. Huang, C. Milliken, *J. Power Sources* 63 (1996) 47.
- [35] L. Kindermann, D. Das, H. Nickel, K. Hilpert, *Solid State Ionics* 89 (1996) 215.
- [36] A.L. Shaula, V.V. Kharton, F.M.B. Marques, A.V. Kovalevsky, A.P. Viskup, E.N. Naumovich, *J. Solid State Electrochem.* 10 (2006) 28.